




# ChromaStarPy: A Stellar Atmosphere and Spectrum Modeling and Visualization Lab in Python

C. Ian Short , Jason H. T. Bayer, and Lindsey M. Burns

Department of Astronomy & Physics and Institute for Computational Astrophysics, Saint Mary's University, Halifax, NS B3H 3C3, Canada; [ian.short@smu.ca](mailto:ian.short@smu.ca)  
Received 2017 September 27; revised 2018 January 8; accepted 2018 January 18; published 2018 February 15

## Abstract

We announce ChromaStarPy, an integrated general stellar atmospheric modeling and spectrum synthesis code written entirely in python V. 3. ChromaStarPy is a direct port of the ChromaStarServer (CSServ) Java modeling code described in earlier papers in this series, and many of the associated JavaScript (JS) post-processing procedures have been ported and incorporated into CSPy so that students have access to ready-made data products. A python integrated development environment (IDE) allows a student in a more advanced course to experiment with the code and to graphically visualize intermediate and final results, ad hoc, as they are running it. CSPy allows students and researchers to compare modeled to observed spectra in the same IDE in which they are processing observational data, while having complete control over the stellar parameters affecting the synthetic spectra. We also take the opportunity to describe improvements that have been made to the related codes, ChromaStar (CS), CSServ, and ChromaStarDB (CSDB), that, where relevant, have also been incorporated into CSPy. The application may be found at the home page of the OpenStars project: <http://www.ap.smu.ca/OpenStars/>.

*Key words:* line: identification – miscellaneous – stars: atmospheres

## 1. Introduction

A refreshing recent development in astronomy research and higher education is the advent of computational tools for commonplace platforms of the type that students are likely to own. This has been enabled by the power and capacity of consumer devices, which now exceed those of institutional workstations of previous decades. This makes it easier to assign lab activities as coursework, and for motivated students to explore computational tools on their own initiative.

The development of the python programming language and of free multi-platform python distributions that include an integrated development environment (IDE), such as spyder, and plotting libraries such as matplotlib (Hunter 2007), has been consequential. The IDE provides an interactive environment for code analysis and development, and a visualization environment similar to that of more established scientific plotting packages. Python is increasingly being used by the observational astronomy community, and there are standard libraries of astronomical procedures such as astropy (Robitaille et al. 2013) and PyRAF (see, for example, de La Peña et al. 2001). An added incentive for python deployments is the advent of notebook applications, such as juPyter, that are equipped with python kernels, and that allow code blocks to be interspersed with marked-up text and plots. The iSpec spectral analysis code (Blanco-Cuaresma et al. 2014) is a recent example of an institutional research capability being made available for more commonly accessible platforms by implementation in python.

We introduce ChromaStarPy (CSPy; DOI: [zenodo.1095687](https://doi.org/10.5281/zenodo.1095687)), a general 1D static plane-parallel LTE atmospheric modeling, spectrum synthesis, and post-processing code written entirely in python, equipped with an optional jupyter notebook interface, and freely available under the MIT license as a source tarball from the home page of the OpenStars project (<http://www.ap.smu.ca/OpenStars>). Additionally, there is a GitHub repository for version-controlled collaborative development (<https://github.com/sevian3/ChromaStarPy>), and we note that the

version numbering scheme is date-based using the ISO 8601 system (YYYY-MM-DD). The code is a direct port of the ChromaStarServer (CSServ) Java application that is described in detail in Short (2016, hereafter S16) and Short (2017, hereafter S17), and its methods and procedures are the same as that code. Like CSServ, CSPy adopts significant modeling approximations to expedite the computation so as to be more suitable for pedagogical application, while retaining a level of modeling realism suitable for projects in a pedagogical context, and for research projects of a carefully limited scope. Given the significance of a port to a more scientific programming language, we take the opportunity to review the methods and major approximations being made in Section 2, present comparisons with observations in Section 3, and in Section 4 we propose sample activities for which CSPy is especially suitable. Related applications that have been described elsewhere include ChromaStarDB (CSDB), a version of CSServ that implements the line list as an SQL database and allows for novel flexibility in selecting or deselecting which spectral lines to include in a spectrum synthesis based on a wide variety of selection criteria (Short 2017), and ChromaStar (CS), a pure JavaScript and html version of the code that uses a small line list of only  $\sim 20$  lines that runs entirely in the client browser and is suitable for broader education and public outreach (EPO; Short 2014). In Section 5 we describe recent improvements to all these related OpenStars codes that have been made since the last published report on those codes, and which, where relevant, are also reflected in CSPy.

## 2. Methods

### 2.1. Atmospheric Structure and Spectrum Modeling

A detailed description of the atmospheric structure modeling and the spectrum synthesis performed by CSServ, and ported to CSPy, including the crucial approximations for expediting the calculation, along with the justifications and discussion of the

limitations, are to be found in S16 and S17. The most significant distinctions from the simplest research-grade modeling are that CSPy obtains the vertical kinetic temperature structure,  $T_{\text{kin}}(\tau)$ , as a function of optical depth,  $\tau$ , by simple rescaling with effective temperature,  $T_{\text{eff}}$ , from one of the three research-grade template models that sample the populated quadrants of the HR diagram, and that the Voigt profiles of spectral lines are approximated with a series expansion (Gray 2005).

CSPy automatically performs a spectrum synthesis calculation after computing the atmospheric structure every time it is run. The code can be run in a “spectrum synthesis” mode in which a previously computed structure is read from an imported source file (a python module), in which case CSPy automatically limits itself to one iteration of the structure to ensure that it has all needed quantities and proceeds quickly to the spectrum synthesis stage. This expedites activities for which the spectrum synthesis parameters should be varied for a fixed atmospheric structure.

### 2.1.1. Line Lists

As of this work CSPy uses a line list of  $\sim 26,000$  atomic lines in the wavelength ( $\lambda$ ) range from 260 to 2600 nm (covering the Johnson *U*, *B*, *V*, *R*, *I*, *J*, *H*, and *K* bands) extracted from the NIST Atomic Spectra Database (Kramida et al. 2015). CSPy expects to read the line list in byte-data form and the distribution includes both the original ascii and the byte-data versions of the line list. The utility procedure LineListPy.py is included with the distribution and converts an ascii line list in the format produced by the Atomic Spectra Database into the byte-data format expected by CSPy. This allows a more advanced user to produce their own custom line lists. Care must be taken to set the numerous output options in the Atomic Spectra Database interface so as to produce an output with fields and units that match what LineListPy.py expects, and some manual post-processing of the ascii output from the database may be necessary to remove special characters. The ascii version of the line list provided with the distribution serves as a template for what is required.

### 2.2. User-defined Two-level Atom

A pedagogically significant additional capability that has been ported from CS is modeling of the energy level populations and the spectral line profile of an artificial atomic species with only two abundant states—a two-level atom (TLA). The user can adjust the abundance of the TLA species on the logarithmic  $A_{12}$  scale used in stellar spectroscopy, and the atomic and line transition data for the TLA. This includes the excitation energy of the lower  $E$ -level ( $E_i$ ), the central wavelength,  $\lambda_o$ , of the spectral line (which, along with the value of  $E_i$ , determines the value of the upper energy level,  $E_j$ ), and the oscillator strength,  $f$ , among other things. The user can ascribe the TLA to any of the first four ionization stages of the corresponding artificial element, and set the first four ionization energies. The user can adjust a pair of “fudge” factors—one for the overall level of the background continuous opacity ( $\kappa_{\lambda}^c$ ; this also affects the overall spectrum synthesis), and the logarithmic enhancement of the Lorentzian wings in the case that the TLA line is saturated. The macroscopic broadening parameters accounting for macro-turbulence and rotation are also applied

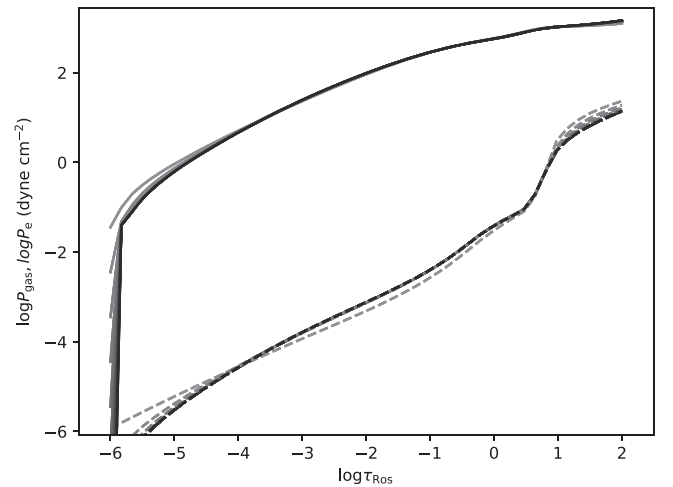


**Figure 1.**  $\log P_{\text{gas}}(\log \tau)$  (solid lines) and  $\log P_e(\log \tau)$  (dashed lines) structures after each of the 12 iterations of the atmospheric structure of a model of  $T_{\text{eff}}/\log g/[\text{Fe}/\text{H}]$  equal to 3600 K/0.0/0.0. Darker lines indicate later iterations. The initial guess consisted of  $\log P_{\text{gas}}(\log \tau)$  and  $\log P_e(\log \tau)$  structures that were approximately rescaled with  $T_{\text{eff}}$ ,  $\log g$ , and  $[\text{Fe}/\text{H}]$  from a template model of 4250 K/2.0/0.0 (see the text).

to the TLA line. CSPy computes the equivalent width,  $W_{\lambda}$ , of the TLA line.

### 2.3. Limb Darkening Coefficients

Like CS, CSServ, and CSDB, CSPy computes monochromatic continuum linear limb darkening coefficients (LDCs),  $\epsilon(\lambda)$ , at each of the  $\lambda$  points sampling the continuum  $I_{\lambda}^c(\lambda, \cos \theta)$  distribution, where  $\theta$  is the angle of emergence of an  $I_{\lambda}$  pencil-beam with respect to the local surface normal, and  $\epsilon$  is defined by the linear limb darkening law,

$$I_{\lambda}^c(\cos \theta)/I_{\lambda}^c(\cos \theta = 1) = (1 - \epsilon) + \epsilon \cos \theta. \quad (1)$$

Currently, CSPy simply solves Equation (1) for  $\epsilon$  separately for each  $(\lambda, \cos \theta)$  pair and averages the resulting  $\epsilon(\cos \theta, \lambda)$  values over  $\cos \theta$  at each  $\lambda$  value to produce  $\epsilon(\lambda)$  values. We plan to eventually replace this with a procedure that finds the best fitting  $\epsilon$  value for the  $I_{\lambda}^c(\cos \theta)/I_{\lambda}^c(\cos \theta = 1)$  values at each  $\lambda$  value.

### 2.4. Comparison to iSpec

iSpec is another astronomical tool for working with model stellar atmospheres and spectra that has been developed in python (see Blanco-Cuaresma et al. 2014), and here we contrast it with CSPy. The iSpec application is an environment that allows a user to make use of libraries of atmospheric models precomputed with research-grade modeling codes, and to compute spectra with their choice of spectrum synthesis codes precompiled from Fortran. This provides a powerful spectral modeling and analysis environment for extracting information from spectra with underlying research-grade modeling codes. By contrast, CSPy is an atmospheric modeling and spectrum synthesis code written entirely in python, and could be run alongside iSpec in a python IDE to generate the synthetic spectra.

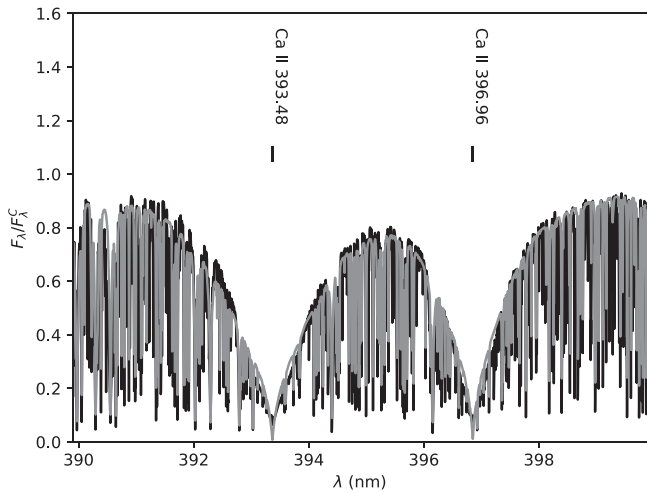


**Figure 2.** Observed Ca II HK region of the solar flux spectrum as presented by Kurucz (2005; black line) and as computed with CSPy (gray line) with a Lorentzian broadening enhancement factor of  $10^{0.5}$ .

### 3. Tests

Figure 1 shows the  $\log P_{\text{gas}}(\log \tau)$  and  $\log P_e(\log \tau)$  structures after each of the 12 iterations of the structure equations for a red supergiant model of  $T_{\text{eff}}/\log g/[\text{Fe}/\text{H}]$  equal to 3600 K/0.0/0.0. For these input parameters, CSPy determined its initial guess at these structures by approximately rescaling from the red giant template of Section 2 (4250 K/2.0/0.0). In addition to demonstrating the convergence properties of our procedure, Figure 1 is a good example of the kind of plot that a student can easily make in a python IDE on their own device by simply instrumenting the code with matplotlib plot statements.

S16 presented comparisons of synthetic spectra computed with CSServ to those computed with Phoenix V. 15 (Hauschildt et al. 1999) for the Ca II region for stars of  $T_{\text{eff}}/\log g/[\frac{\text{Fe}}{\text{H}}]/\xi_T$  equal to 5000 K/4.5/0.0/1.0 km s<sup>-1</sup> and 5000 K/2.5/0.0/1.0 km s<sup>-1</sup>, and the Mg II  $\lambda$  4481 region for a model of 10,000 K/4.0/0.0/1.0 km s<sup>-1</sup>. As of S16, we were not yet ready to compare synthetic and observed spectra in the vicinity of H I lines for early-type stars because we had not yet incorporated linear Stark broadening for the Balmer lines, and the Mg II  $\lambda$ 4481 line is the next most important MK classification diagnostic for these stars. S17 presented the equivalent comparisons for the TiO  $C^3\Delta - X^3\Delta$  ( $\alpha$  system, band origin,  $\lambda_{00} = 517.02$  nm) and  $c^1\Phi - a^1\Delta$  ( $\beta$  system,  $\lambda_{00} = 560.52$  nm) bands for stars of solar metallicity of  $T_{\text{eff}} = 3750$  K and  $\log g$  values of 4.5 and 2.0, and of  $T_{\text{eff}} = 4250$  K and  $\log g = 2.0$ .

Figure 2 shows the flux spectrum,  $F_\lambda$ , of the Sun in the heavily blanketed Ca II HK region based on observations with a resolving power,  $R$ , of 300,000 described by Kurucz (2005), and as computed with CSPy with a Lorentzian broadening enhancement factor of  $10^{0.5}$ . We note that the NIST atomic line list is much less complete than current competitive research-grade line lists, and we do not expect to completely treat the line blanketing in this region. We adopt the standard parameters of  $T_{\text{eff}} = 5777$  K,  $\log g = 4.44$ , and  $[\text{Fe}/\text{H}] = 0.0$ , and a value of the microturbulent velocity dispersion,  $\xi_T$ , of 1 km s<sup>-1</sup>. Figure 3 shows the same region for Arcturus ( $\alpha$  Boo, HD124897, HR5340, K1-K1.5 III) as observed by Hinkle & Wallace (2004) at  $R \approx 100,000$  and as computed with CSPy. We adopt the parameters of Griffin & Lynas-Gray

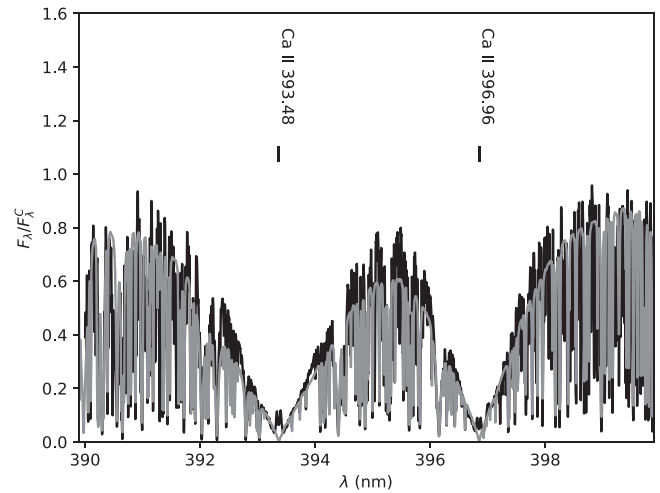


**Figure 3.** Ca II HK region of the flux spectrum of Arcturus ( $\alpha$  Boo) as observed by Hinkle & Wallace (2004; black line) and as computed with CSPy (gray line) with no Lorentzian broadening enhancement. We note that our models do not have a chromospheric temperature inversion and we do not expect to fit the core emission reversals in the strong HK lines.

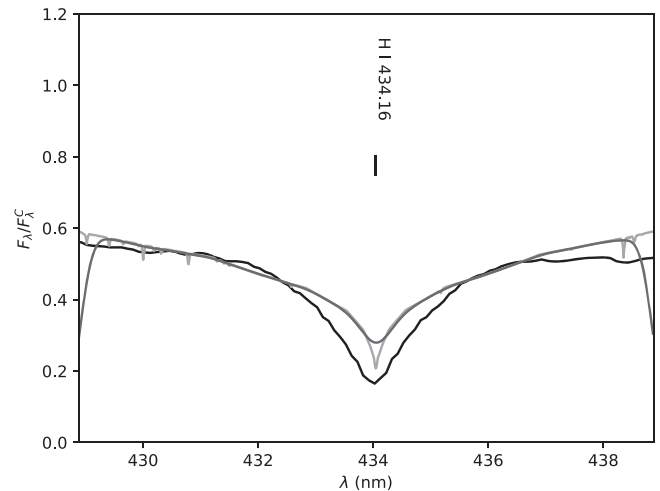


**Figure 4.** H I Balmer  $\gamma$  region of the flux spectrum of Vega ( $\alpha$  Lyr) as observed by Le Borgne et al. (2003; black line) and as computed with CSPy (light gray line), and then instrumentally broadened to  $R = 2000$  (dark gray line). We note that we expect to fit the far wings of the linear Stark broadening profile with our current treatment.

(1999), rounded to to the nearest canonical values,  $T_{\text{eff}} = 4300$  K,  $\log g = 2.0$ , and  $[\text{Fe}/\text{H}] = -0.7$ , with an  $\alpha$ -process element enhancement of  $+0.3$  (Peterson et al. 1993), and adopt a value of  $\xi_T$  of 2 km s<sup>-1</sup>. Because our scaled radiative and convective thermal equilibrium models lack a chromospheric temperature inversion, we do not expect to reproduce the emission core reversals that are apparent in the observed spectrum of Arcturus. Because of the high spectral resolution of the observational material, and the approximate nature of the modeling that we are assessing, we make no attempt to convolve the synthetic spectra to match the instrumental resolution of the observations.

Figure 4 presents a comparison of the H I H $\gamma$  wings for Vega ( $\alpha$  Lyr, HD 172167, HR 7001, A0 V) as observed by Le Borgne et al. (2003) at  $R \approx 2000$ , and as computed with CSPy and broadened by convolution with a Gaussian kernel to the  $R$  value of the observed spectrum. H $\gamma$  is the longest wavelength Balmer line in the observed spectrum, and we chose it for

comparison because we expect it to be the least blended with neighboring lines. We adopt the parameters of Castelli & Kurucz (1994) of  $T_{\text{eff}} = 9550$  K,  $\log g = 3.95$ ,  $[\text{Fe}/\text{H}] = -0.5$ , and  $\xi_T = 2$  km s<sup>-1</sup> for the structure, and values of  $v_{\text{rot}}$  and  $i$  of 275 km s<sup>-1</sup> and 5°, respectively, corresponding to a  $v \sin i$  value of 24 km s<sup>-1</sup> (Peterson et al. 2006), for the post-processing of the spectrum. We note that currently we only treat linear Stark broadening in the far wing, as described in S17, for  $\Delta\lambda > 2\Delta\lambda_D$ , where  $\Delta\lambda_D$  is the Doppler width, and only expect to match the profile approximately in that regime.

#### 4. Applications

As an integrated stellar atmospheric modeling and spectrum synthesis code, CSPy takes as input the standard parameters needed for unblanketed, static, 1D, plane-parallel, LTE, scaled-solar abundance modeling:  $T_{\text{eff}}$ ,  $\log g$ , and  $[\text{Fe}/\text{H}]$ . Because this is a pedagogical code, it also allows the user to specify a stellar mass,  $M$ , which it uses to compute and display the stellar radius,  $R$ , and bolometric luminosity,  $L_{\text{bol}}$ , corresponding to the values of  $T_{\text{eff}}$  and  $\log g$ . It also requires parameters specifying the spectrum synthesis: the wavelength range,  $[\lambda_1, \lambda_2]$ , the microturbulent velocity dispersion,  $\xi_T$ , fudge factors for tuning the background continuum opacity,  $\kappa_{\lambda}^c$ , and the Lorentzian line broadening. Because post-processing of the spectrum accounting for natural effects is integrated, it also allows specification of the macroturbulent dispersion,  $\xi_{\text{Macro}}$ , the surface equatorial rotation velocity,  $v_{\text{rot}}$ , and the inclination of the rotation axis to the line-of-sight,  $i$ .

Because python is an interpreted rather than a compiled language, it allows for flexible diagnostic interaction when running in an IDE such as spyder. The values of intermediate variables can be inspected, ad hoc, at the console prompt. When accompanied by a plotting facility, such as matplotlib, the code can be instrumented with ad hoc plot statements that allow for visual inspection of how various structures are converging from one iteration to the next, as exemplified by Figure 1. Students can edit the code and rerun it while learning about or developing the code. As a result, the IDE is effectively an integrated computational astrophysics lab bench.

Students can post-process the synthetic spectra with operations such as convolution in the IDE. Students in observational astronomy courses who have acquired a sample observed stellar spectrum can import the observational data into the IDE and compare it, qualitatively or statistically, to suitably post-processed model spectra generated ad hoc with various trial stellar and spectrum synthesis parameters. Students can extract the  $W_{\lambda}$  value of a spectral line, either with the built-in procedure if they restrict the synthesis range to isolate one line, or with a python procedure of their own. A local example is that students in the fourth year observational astronomy or experimental physics courses in our program at Saint Mary's University can acquire CCD spectra with the spectrograph on the 60 cm telescope of the Burke-Gaffney Observatory (BGO), and compare model spectra produced with CSPy in a python IDE.

##### 4.1. TLA

The TLA (see Section 2.2) can be used to study the simple curve-of-growth (COG) of a spectral line, which, here, is effectively being defined as  $\log W_{\lambda}([\text{A}/\text{H}])$ . Because the TLA is treated with a Voigt profile, the COG will exhibit

the weak, strong, and saturated regimes as  $[\text{A}/\text{H}]$  increases. The student can experimentally investigate how the COG varies with  $f$  and  $E_i$ .

The TLA can be used to model specific real spectral lines that are important diagnostics. An effective example is to set the TLA parameters to those of the Ca I  $\lambda 4227$  line, and then the Ca II K line, and to study the  $\log W_{\lambda}(T_{\text{eff}})$  behavior over the  $T_{\text{eff}}$  range of late-type stars (3500–6500 K). This provides a good example of the role that ionization equilibrium plays in the relation between  $T_{\text{eff}}$  and the MK spectral class.

#### 5. Improvements to the OpenStars Suite

A number of significant improvements to the related codes CS, CSServ, and CSDB have been made since our last report, and these have also been incorporated into CSPy where relevant.

##### 5.1. Partition Functions

As of S17, CS, CSServ, and CSDB estimated the value of the partition function,  $U_i(\theta)$ , for species  $i$  by linear interpolation among two values of  $\theta$ , 0.5, and 1.0, where  $\theta \equiv 5040/T$ , with the  $U_i(\theta)$  values taken from Cox (2002). The treatment has been improved by interpolating in  $T$  among the  $U_i(T)$  values of Barklem & Collet (2016) for  $T$  values of 130, 500, 3000, 8000, and 10,000 K. We incorporate the  $T$  values below 3000 K in anticipation of eventually adapting the modeling so as to be more suitable for brown dwarfs. For now, the interpolation in  $T$  remains linear, but this new treatment yields  $n_i(\tau)$  distributions that are more continuous and do not suffer from the small discontinuities that were produced by the two-temperature  $U_i(\theta)$  treatment.

##### 5.2. Non-solar Abundance Distributions

In addition to allowing for adjustment of the overall scaled-solar metallicity,  $[\text{Fe}/\text{H}]$ , the codes now also allow the user to independently adjust the values of the logarithmic quantities  $[\text{He}/\text{Fe}]$ ,  $[\alpha/\text{Fe}]$ , and  $[\text{C}/\text{O}]$ , where  $\alpha$  indicates eight  $\alpha$ -process elements (O, Ne, Mg, Si, S, Ar, Ca, and Ti). This affects the computation of the  $P_{\text{gas}}(\tau)$  and  $P_e(\tau)$  structures through the EOS and HSE treatment, and the value of the background  $\kappa_{\lambda}(\tau)$  distribution, as well as having a direct effect on the strengths of the relevant lines in the spectrum synthesis. This allows the user to investigate the effect on both the atmospheric structure and spectrum of He enrichment in A and B stars,  $\alpha$ -enhancement in metal-poor RGB stars, and enhanced C/O values in post-dredge-up AGB stars.

##### 5.3. Photometry

The Johnson *UBVRI* filters employed by the integrated post-processing suite have now been supplemented with the *HJK* filters, and we have adopted the response curves of Johnson (1965), as reported in the Asiago Database of Photometric Systems (Moro & Munari 2000). The SED is now computed from 260 to 2600 nm, and the additional filters allow us to compute and display the standard  $V - K$  and  $J - K$  color indices. These are relevant as our modeling currently extends down to  $T_{\text{eff}}$  values of 3400 K, and will become increasingly important as we extend our treatment to even lower  $T_{\text{eff}}$  values.

### 5.4. H Lines

CS is the version of the code that is implemented entirely in JavaScript, and necessarily has a very limited line list of 20 lines, and only included the Balmer series lines of H I up to H $\epsilon$ . Now that the SED is computed and displayed for  $\lambda < 364$  nm, we have added two additional H lines, H(2–8) and H(2–9), and a user who has their own installation can uncomment an additional eight H lines, up to H(2–17). The H line treatment includes Stark broadening, and these higher Balmer lines allow for a somewhat more realistic treatment of the SED for  $\lambda \geq 364$  nm.

### 5.5. Scalable Vector Graphics

As of our last report, CS used the HTML5  $\langle$ canvas $\rangle$  element for the graphical output. This is not scale invariant, and the alphanumeric graphical elements were not sharp at any zoom setting, and became increasingly pixelated in appearance at the higher zoom setting sometimes required for accurate lab work. We now use the HTML5  $\langle$ SVG $\rangle$  (scalable vector graphics) element for the output and the graphical elements now remain sharp at all zoom settings. Moreover, the  $\langle$ SVG $\rangle$  element allows for interactivity based on event handlers to be added to the graphics, and we have taken advantage of this to provide the UI with additional functionality that will help make the application more enticing at a basic level of pedagogy and outreach:

1. On all plots, when the user hovers, the data coordinates are displayed and this allows for more precise quantitative information to be extracted from the plots.
2. The user can now set the input stellar parameters by clicking on the HR diagram.
3. The user can now tune the narrow band filter by clicking on the rendering of the spectral image.

## 6. Discussion

CSPy fills a gap between the research-grade stellar atmosphere and spectrum synthesis codes that are compiled from fortran and require a unix-like environment, and the web-browser based pedagogical modeling of CS, CSServ, and CSDB. Because python has a well-developed set of support tools such as IDEs, signal processing, and plotting libraries, CSPy is a unique lab for studying and developing an astrophysical modeling code at the senior undergraduate or introductory graduate level in an interactive and graphical way on common student-owned devices.

Python supports multi-threaded programming, and many commonplace devices now have multi-core CPUs, so the way is open for improving the performance of CSPy and other modeling codes in python, and enabling more realistic modeling in a pedagogically engaging environment. Now that the code has been ported to python, it would be relatively straightforward to port it to Julia, a language with a similar syntax that has been receiving increasing attention recently. Julia is also an interpreted language, and so also offers the flexibility and transparency of an interpreted development and

run-time environment, but promises to yield executable code that runs significantly faster than that of python. Execution speed is one of the main advantages that compiled languages like fortran have over interpreted languages, so a port of ChromaStarPy to Julia could be significant.

More generally, the OpenStars project is based on the philosophy that if it is worth computationally modeling an astronomical object for research purposes, then it is also worth using the model to render what the object looks like in ways that people outside the research community, or who are learning the subject at a more basic level, will find intuitive and relatable, and can interact with. Commonplace computing technology now allows for this, and this represents a new way for the astronomy research and higher education community to be relevant beyond the research and higher education institutions. We continue to encourage computational astrophysicists to consider didacticizing the modeling and visualization that they do and deploying it in forms that are relevant to education and public outreach.

The authors acknowledge the Natural Sciences and Engineering Research Council of Canada (NSERC) grant RGPIN-2014-03979. The authors also thank Saint Mary's Astronomy graduate students Mitchell Young and Diego Castañeda for valuable guidance on python distributions.

### ORCID iDs

C. Ian Short  <https://orcid.org/0000-0003-4045-128X>

### References

- Barklem, P. S., & Collet, R. 2016, *A&A*, **588**, A96
- Blanco-Cuaresma, S., Soubiran, C., Heiter, U., & Jofre, P. 2014, *A&A*, **569**, 111
- Castelli, F., & Kurucz, R. L. 1994, *A&A*, **281**, 817
- Cox, A. N. (ed.) 2002, *Allen's Astrophysical Quantities* (4th ed.; Berlin: Springer)
- de La Peña, M. D., White, R. L., & Greenfield, P. 2001, in *ASP Conf. Proc.* 238, *Astronomical Data Analysis Software and Systems X*, ed. F. R. Harnden, Jr., F. A. Primini, & H. E. Payne (San Francisco, CA: ASP), 59
- Gray, D. F. 2005, *The Observation and Analysis of Stellar Photospheres* (3rd ed.; Cambridge: Cambridge Univ. Press)
- Griffin, R. E. M., & Lynas-Gray, A. E. 1999, *AJ*, **117**, 2998
- Hauschildt, P. H., Allard, F., Ferguson, J., Baron, E., & Alexander, D. R. 1999, *ApJ*, **525**, 871
- Hinkle, K. H., & Wallace, L. 2004, *BAAS*, **36**, 1423
- Hunter, J. C. 2007, *CSE*, **9**, 90
- Johnson, H. L. 1965, *ApJ*, **141**, 923
- Kramida, A., Ralchenko, Y., Reader, J. & NIST ASD Team 2015, *NIST Atomic Spectra Database ver.5.3* (Gaithersburg, MD: National Institute of Standards and Technology), <http://physics.nist.gov/asd>
- Kurucz, R. L. 2005, *MSAIS*, **8**, 189
- Le Borgne, J.-F., Bruzual, G., Pello, R., et al. 2003, *A&A*, **402**, 433L
- Moro, D., & Munari, U. 2000, *A&A*, **147**, 361
- Peterson, D. M., Hummel, C. A., Pauls, T. A., et al. 2006, *Natur*, **440**, 896
- Peterson, R. C., Dalle Ore, C. M., & Kurucz, R. L. 1993, *ApJ*, **404**, 333
- Robitaille, T. P., Tollerud, E. J., Greenfield, P., et al. 2013, *A&A*, **558**, 33
- Short, C. I. 2014, *JRASC*, **108**, 230
- Short, C. I. 2016, *PASP*, **128**, 104503
- Short, C. I. 2017, *PASP*, **129**, 094504